VIP Upconversion Very Important Paper

Deutsche Ausgabe: DOI: 10.1002/ange.201510609
Internationale Ausgabe: DOI: 10.1002/anie.201510609

Filtration Shell Mediated Power Density Independent Orthogonal Excitations–Emissions Upconversion Luminescence

*Xiaomin Li[+], Zhenzhen Guo[+], Tiancong Zhao, Yang Lu, Lei Zhou, Dongyuan Zhao, and Fan Zhang**

Abstract: *Lanthanide doped core–multishell structured $NaGdF_4$:Yb,Er@$NaYF_4$:Yb@$NaGdF_4$:Yb,Nd@$NaYF_4$@-$NaGdF_4$:Yb,Tm@$NaYF_4$ nanoparticles with power-density independent orthogonal excitations-emissions upconversion luminescence (UCL) were fabricated for the first time. The optical properties of these core–multishell structured nanoparticles were related to the absorption filtration effect of the $NaGdF_4$:Yb,Tm layer. By tuning the thickness of the filtration layer, the nanoparticles can exhibit unique two independent groups of UCL: Tm^{3+} prominent UV/blue (UV = ultraviolet) UCL under the excitation at 980 nm and Er^{3+} prominent green/red UCL under the excitation at 796 nm. The filtration-shell mediated orthogonal excitations-emissions UCL are power-density independent. As a proof of concept, the core–multishell nanoparticles are used in multi-dimensional security design and imaging-guided combined photodynamic therapy and chemotherapy.*

Lanthanide-doped upconversion nanoparticles (UCNPs) represent a class of luminescent nanomaterials being developed as a promising alternative to organic dyes and quantum dots. As the most prominent feature, a single nanoparticle can incorporate a combination of lanthanide dopant ions that produce excitons of distinct energies, thereby giving rise to highly designable emission profiles.[1] Significantly, core–shell structural engineering has emerged as a powerful means to construct novel UCNPs by integrating functionalities and regulating the complex interplay of lanthanide interactions, these interactions can be used to easily access to UCNPs with well-defined phase and size, surface properties, especially optical emission.[2] These advances provide promising applications in sensitive biodetection and advanced bioimaging without many of the constraints associated with conventional optical biolabels.[3] One of the critical requirements for harvesting their full potential is to develop lanthanide-doped nanoparticles with emission profiles specifically tuned toward their target applications. Among the various developed UCNPs with tailored emission profiles, multicolor emission nanoparticles capable of regulating their emission wavelengths from the UV to visible range in response to external stimuli are garnering more and more interest, as they can offer more dynamic platforms for applications in multicolor encoding, photoswitching, and high-resolution bioimaging.[4] However, there are only a few reports on orthogonal excitations-emissions, that is, an excitation-responsive luminescence, whose emission can be modulated between different luminescence events of different lanthanide activators by changing the excitation wavelength.[2d,5] This unique property of the nanoparticles has been applied toward driving chemical reactions and their subsequent applications, such as two-way photoswitching of spiropyran and dithienylethene,[5a,b] reversible control over modulating the biocatalytic activity of bacteria,[5c] and reflection of liquid crystals.[5d] Despite current strategies for orthogonal excitations-emissions UCL, most of them are based on tuning of the excitation power density,[5] which could induce severe local heating under the high power density. In addition, the emission colors are not fixed under different excitation power density. Thus, to overcome these limitations, it is desirable to develop power density-independent orthogonal excitations-emissions UCNPs.

Herein, power-density-independent orthogonal excitations-emissions $NaGdF_4$:Yb,Er@$NaYF_4$:Yb@$NaGdF_4$:Yb,Nd@$NaYF_4$@$NaGdF_4$:Yb,Tm@$NaYF_4$ core–multishell structured UCNPs were synthesized for the first time. By tuning the thickness of the absorption filtration layer ($NaGdF_4$:Yb,Tm), the core–multishell structured UCNPs can exhibit two groups of independent orthogonal excitations-emissions UCL: Tm^{3+} prominent UV/blue UCL under the excitation at 980 nm and Er^{3+} prominent green/red UCL under the excitation at 796 nm. The filtration shell mediated orthogonal excitations-emissions UCL are power-density independent. The unique optical properties allow these core–multishell nanoparticles to be used in multi-dimensional security design (patterns, emissions, and excitations). Combined with the superiority of mesoporous silica ($mSiO_2$) nanoparticles, the hollow structured UCNPs@$mSiO_2$ can also be used for the near infrared (NIR) to NIR downconversion luminescence (DCL) bioimaging-guided photodynamic and chemotherapy combined treatment by using the green/red and UV/blue UCL.

The C-S1-S2-S3-S4-S5 (C = core; S = shell) nanostructure platform is designed for 796 nm and 980 nm light harvesting by controlling the energy-transfer processes of the dopants and optical tuning processes at separate layers (Figure 1 A,B). Each of the layers has a different component and controllable thickness. Each layer assumes a specific role and they all work

[*] Dr. X. Li,[+] Z. Guo,[+] T. Zhao, Y. Lu, L. Zhou, Prof. D. Zhao, Prof. F. Zhang
Department of Chemistry and Laboratory of Advanced Materials
State Key Laboratory of Molecular Engineering of Polymers, Collaborative Innovation Center of Chemistry for Energy Materials (2011-iChEM), Fudan University
Shanghai 200433, (P.R. China)
E-mail: zhang_fan@fudan.edu.cn

[+] These authors contributed equally to this work.

Supporting information for this article is available on the WWW under http://dx.doi.org/10.1002/anie.201510609.

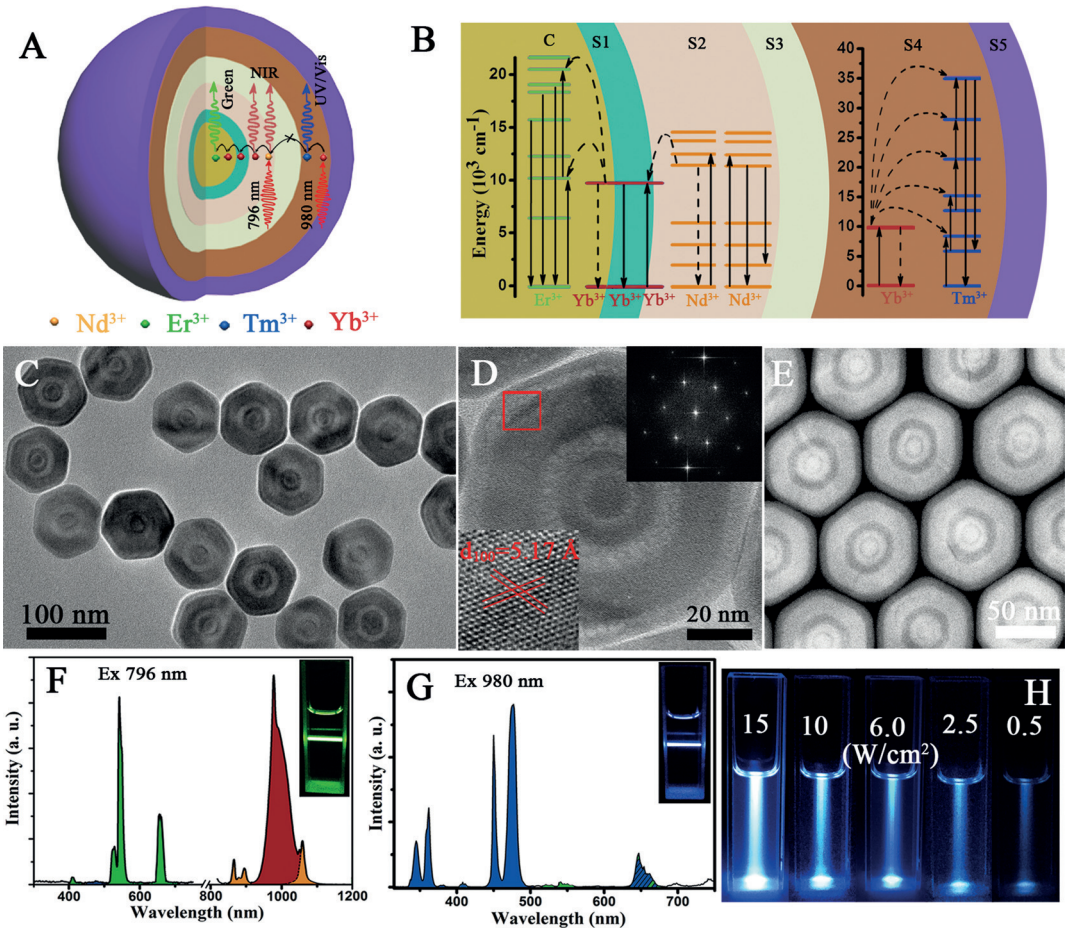

Figure 1. The structure (A) and energy-transfer mechanisms (B), TEM (C), HRTEM and the corresponding FFT (D), HAADF-STEM (E) of the orthogonal excitations-emissions UCNPs. The UCL spectra of the UCNPs under the excitation of 796 nm (F) and 980 nm (G). H) Digital camera photographs of the UCNPs under different excitation-power-density 980 nm excitations.

together to give the unique power-density-independent orthogonal excitations-emissions UCL. This nanostructure can be divided into four parts (Figure 1 B): the C-S1-S2 structured $NaGdF_4$:Yb,Er @$NaYF_4$:Yb@$NaGdF_4$:Yb,Nd for the Er^{3+} dominated green/red UCL under 796 nm excitation; $NaGdF_4$:Yb,Tm (S4) for the Tm^{3+} prominent UV/blue UCL under 980 nm excitation, which can also work as the shell thickness dependent absorption-filtration layer for tuning the Er^{3+} dominated UCL in the inner core; $NaYF_4$ (S3) for the energy-transfer barrier between the green emission and blue emission layers; outmost $NaYF_4$ (S5) layer for minimizing the defects and external deactivators. Because the 796 nm excited UCL is more sensitive to the surrounding environment than that of excited by 980 nm , the 796 nm excited C-S1-S2 part is placed in the inner most section of the core–multishell structure. In the C-S1-S2 part, the Nd^{3+} ions confined in S2 serve as the sensitizer to harvest 796 nm photons. The Yb^{3+} ions in S2 and S1 are used to extract the excitation energy from the sensitizer Nd^{3+} through interionic cross-relaxation, followed by excitation-energy migration over the Yb sublattice and finally entraped by the Er^{3+} activator ions embedded in the inner core. In the S4 part, the energy harvested by the Yb^{3+} sensitizers are transferred to Tm^{3+} through the classical energy transfer upconversion process to realize the UV/blue UCL under 980 nm excitation. The S4 layer is also used as the absorption filtration layer as a result of the strong absorption of Yb^{3+} for 980 nm light. By tuning the thickness of the S4 filtration layer the dose of 980 nm irradiation arriving at the inner most $NaGdF_4$:Yb,Er can be controlled.

Transmission electron microscopy (TEM) images show discernible contrast for the core–multishell nanostructure of the as-prepared nanoparticles and an apparently uniform size and morphology with an average diameter of approximately 19 nm, 30 nm, 45 nm, 70 nm, 85 nm after S1, S2, S3, S4, and S5 coating (Figure 1 C, Figure S1 in the Supporting Information). The high-resolution TEM image along with the corresponding fast Fourier transform (FFT, Figure 1 D) of the resultant nanoparticles show that the nanoparticles are highly crystalline hexagonal phase without any significant impurity phases. The high-angle annular darkfield scanning TEM (HAADF-STEM) was also employed to identify the formation of the core-multishell structures (Figure 1 E, Figure S2–S5), in which the brighter regions correspond to heavier elements (Gd, Yb, and Nd) and the darker parts correspond to the lighter one (Y).

Generally, the UCLs dominated by different activators (Tm^{3+}, Er^{3+}, etc.) in the core–shell structure are always

symbiotic under fixed excitation.[6] It is very difficult to make them emit their characteristic emissions independently, especially under excitation at 980 nm. To obtain the orthogonal excitations-emissions UCL, the most commonly used strategy is based on the tuning of the excitation power density[5] or the doping concentration,[5d] which could induce severe local heating and decrease the absolute luminescence intensity, respectively. In addition, the emission color is not fixed under different excitation power density. In our structure, power density independent orthogonal excitations-emissions can be realized by accurate control of the thickness of the absorption filtration layer. Owing to the presence of the S3 $NaYF_4$ energy barrier layer, the energy transfer between S2 and S4 is blocked, and the green UCL under 796 nm excitation is from the Er^{3+} (Figure 1F). Normally, this Er^{3+} activator sensitized by Yb^{3+} in the inner core may also be excited under 980 nm excitation. However, owing to the absorption filtration effect of S4, nearly pure Tm^{3+} dominated UCL can be obtained under excitation at 980 nm (Figure 1G). Interestingly, the blue emission color does not change under different power density of 980 nm irradiations, meaning that the filtration shell mediated orthogonal excitations-emissions UCLs are power density independent.

To further investigate the two independent groups of UCL of the core–multishell nanoparticles at a single particle level (Figure S6), dilute samples were dispersed on pretreated glass substrates and imaged in an optical microscope equipped with an electron-multiplying charge-coupled device camera while excited with a tightly focused 980 nm laser (Figure S7). Photoluminescent images of the samples revealed homogeneous and randomly distributed diffraction-limited spots at the microscale corresponding to single particles. The local in situ spectral analyses of the luminescent spots show that the nanoparticles can also exhibit orthogonal excitations-emissions on the microscale (Figure S6). The photoluminescence time traces under continuous illumination with different excitations reveals that the sample has long-term stability and no photoblinking was detected when the bin time for each data point in emission intensity was reduced to 100 ms (Figure S8).

As mentioned above, the thickness of the filtration $NaGdF_4$:Yb,Tm S4 layer in our core–multishell structure is very important for tuning the intensity of Er^{3+} emission. Clearly, the emissions of the Er^{3+} in the inner core are depressed gradually as the thickness of S4 increases from approximately 5 nm to 15 nm,[7] the color of the luminescence changes from Er^{3+} dominated green emission to Tm^{3+} dominated blue emission (Figure 2C). We assume that the suppression of the Er^{3+} emission is mainly a result of the filtration effect of the S4 layer. The 980 nm light is nearly exhausted by the absorption of Yb^{3+} in the S4 layer before it can be used to excite the UCL of Er^{3+} in the inner-most core. More interestingly, the nanoparticles have a disk shape (Figure S9), which means the filtration effect of the shell is anisotropic for the inner core. The anisotropic filtration is in agreement with the polarization of UCL of hexagonal nanodisks,[8] which can further induce the suppression of Er^{3+} emission. Compared with the pure green emission under the 980 nm excitation from $NaGdF_4$:Yb, Tm@$NaYF_4$:Yb@$NaGdF_4$:Yb,Nd@$NaYF_4$@$NaGd_4$:Yb,Er@ $NaYF_4$ nanoparticles (Figure S10), the above mentioned pure blue emission is more difficult, because the inherent UCL process of Er^{3+} is always much easier than that of Tm^{3+}. Thus the pure blue emission further demonstrates the effectiveness of the filtration shell.

Figure 2D shows the 980 nm excitation-power dependence of UCL intensities of typical core-multishell structured nanoparticles (with both Er^{3+} and Tm^{3+} character emissions; the thickness of the S4 absorption-filtration layer is about 10 nm). By increasing excitation power density from 0.5 to 15 $W cm^{-2}$, the green, blue, and red emissions increased accordingly. The slopes of ln–ln plots of emission intensity versus 980 nm excitation power show that the plots for 475 nm, 542 nm, 640 nm are nearly parallel with each other (Figure 2E), indicating the relative intensity among blue (475 nm), green (542 nm) and red (640 nm) emissions remains at different excitation power density (Figure 2F). In other words, the emission colors under 980 nm excitation are independent on the power density (Figure 1H), which is quite different from the previous reports.[5a–c] But for the emission at 360 nm, the intensity sharply increases with increasing the excitation power density, which means that the multiphoton upconversion process in Tm^{3+} is promoted under high excitation power density. Thus, we think that the multiphoton upconversion process of Tm^{3+} can further increase the absorption-filtration effect of S4, especially at high excitation power density.

The quantum efficiency of UCL is much lower than DCL emitted by lanthanide-doped nanoparticles. Thus, the Nd^{3+} and Yb^{3+} in S2 dominated NIR DCL can be obtained under the low excitation power density of 796 nm (< 0.5 $W cm^{-2}$; Figure 2G). The irradiation power density dependent emission intensity of the NIR DCL (976 nm) and green UCL (542 nm) show that the two emissions are always present concurrently under high excitation power density (> 0.5 $W cm^{-2}$, Figure 2G). The UCL nearly disappears when power density is lower than 0.5 $W cm^{-2}$, which is small enough to avoid local heating. In comparison, the efficiency of Nd^{3+} and Yb^{3+} dominated DCL is much higher than that of UCL, which is consistent with literature reports.[11] The relative intensity between the DCL and UCL gradually increases with decreasing the power density (Figure 2H,I).

Taking advantage of the significant orthogonal excitations-emissions properties, a multi-dimensional (patterns, emissions, and excitations) security marking was designed by using the core-multishell nanoparticles (Figure 3A). A dispersion of nanoparticles in cyclohexane was used as cryptographic ink to directly write on the paper. In daylight, the pattern word on the paper was invisible. As expected, upon 796 nm excitation , a bright green "FD" pattern was observed on the paper. The color pattern changed to blue with the excitation at 980 nm. Significantly, the emission color of the pattern is independent of the excitation power density, which is consistent with the UCL spectra (Figure 2D–F). Furthermore, under the low excitation power density of 796 nm, the visible green pattern disappeared and was displaced by the pattern with NIR emission. This unique

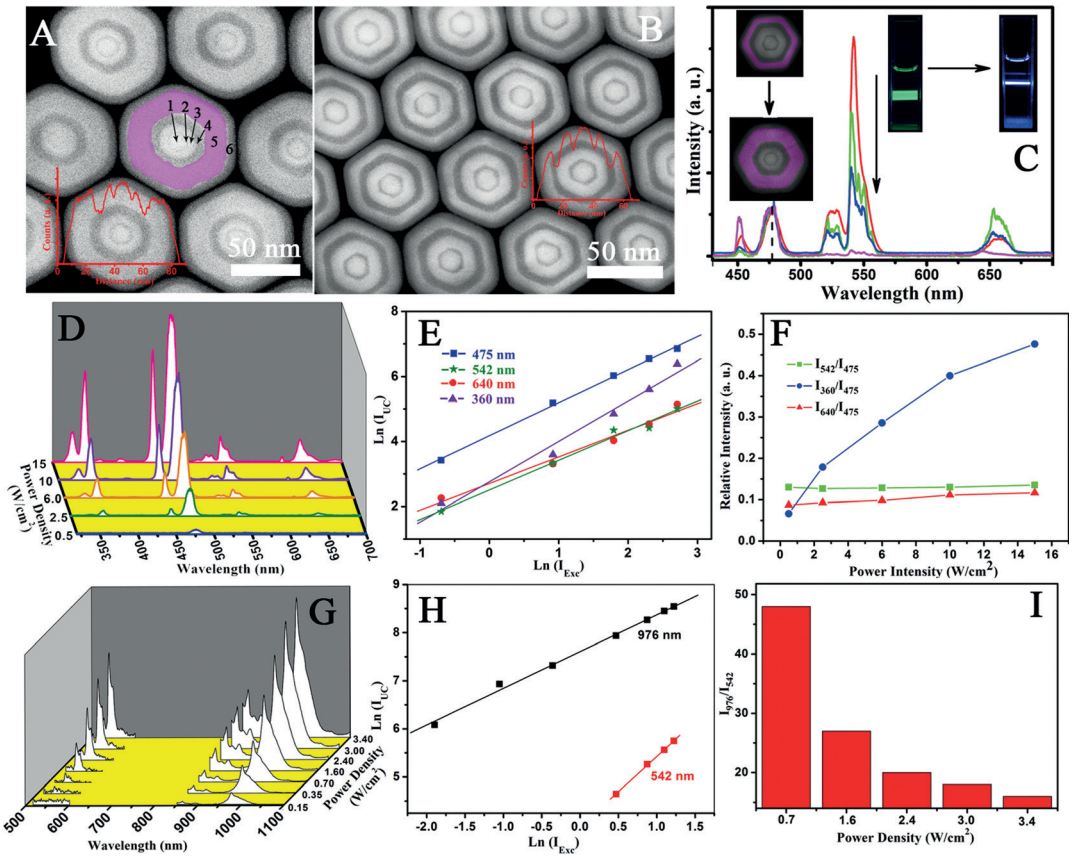

Figure 2. HAADF-STEM with line profile analysis of image gray level (A,B) and UCL spectra under the irradiation of 980 nm (C, red: 5 nm; green: 7 nm; blue: 10 nm; purple: 15 nm; inset: typical HAADF-STEM images (left) and photographs under 980-nm excitation (right) of the nanoparticles with 5 nm and 15 nm of S4) of the core-multishell nanoparticles with different thickness of S4; D),G) Pump-power-dependent UCL and DCL emission spectra of typical core-multishell structured nanoparticles (with both Er^{3+} and Tm^{3+} character emissions, the thickness of S4 absorption-filtration layer is about 10 nm); Irradiation-power-density-dependence emission intensity (E,H) and relative intensity of different emission bands (F,I) under different irradiation.

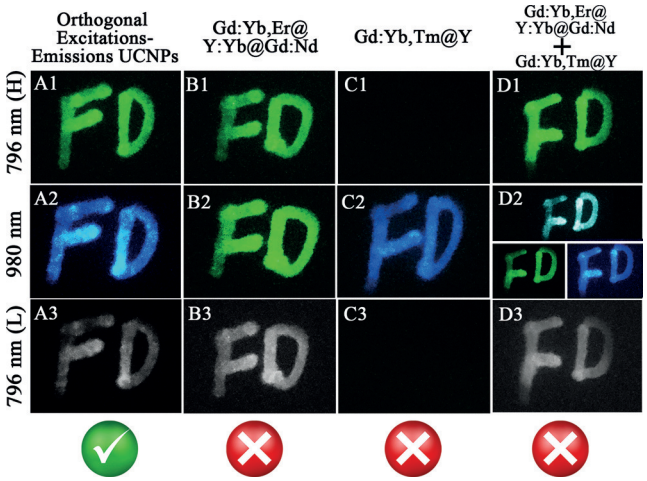

Figure 3. Anti-counterfeiting luminescence images of the orthogonal excitations-emissions $NaGdF_4$:Yb,Er@$NaYF_4$:Yb@$NaGdF_4$:Yb, Nd@$NaYF_4$@$NaGdF_4$:Yb,Tm@$NaYF_4$ (A), $NaGdF_4$:Yb,Er@$NaYF_4$: Yb@$NaGdF_4$:Yb,Nd (B), $NaGdF_4$:Yb,Tm@$NaYF_4$ (C) and the mixture of $NaGdF_4$:Yb,Er@$NaYF_4$:Yb@$NaGdF_4$:Yb,Nd and $NaGdF_4$:Yb, Tm@$NaYF_4$ (D) UCNPs under different excitations (H and L means high and low power densities, respectively). Photographs shown in D2 are the original luminescence images and the luminescence images with green and blue optical filters.

property cannot be imitated by any other upconversion nanoparticles species (Figure 3A,C) or the mixture of them (Figure 3D).

Combined with $mSiO_2$ nanoparticles, hollow structured UCNPs@$mSiO_2$ (Figure 4A,C, S9, S11, S12) can also be used for bioimaging-guided combined photodynamic and chemotherapy treatment. In this nanocomposite, the NIR DCL under low power density 796 nm ($<0.5\ W\,cm^{-2}$) excitation is used as a bioimaging signal (Figure 4B), the green-emission-triggered photodynamic therapy (PDT) cannot work under these conditions. However, through the consistency between the UV/blue emission and the absorption of the light sensitive azobenzene (Azo) nanoimpeller (the transformation between the *cis*-isomer and *trans*-isomer of Azo can work like a impeller to drive the release of guest) (Figure 4D),[9] Tm^{3+} dominated UV/blue emission under 980 nm excitation could be used to trigger the release of the chemotherapy drug. The reversible photoisomerization caused by the simultaneous emission of UV/blue light from the UCNPs and the photothermal effect of 980 nm light creates a continuous rotation–inversion movement, which can be used to trigger the release of the encapsulated chemotherapy drug.[10] Independently, the PDT can also be realized under the stimulus of green emission excited by 796 nm under high power density ($>0.5\ W\,cm^{-2}$). Rose Bengal (RB) was used as the photosensitizing molecule

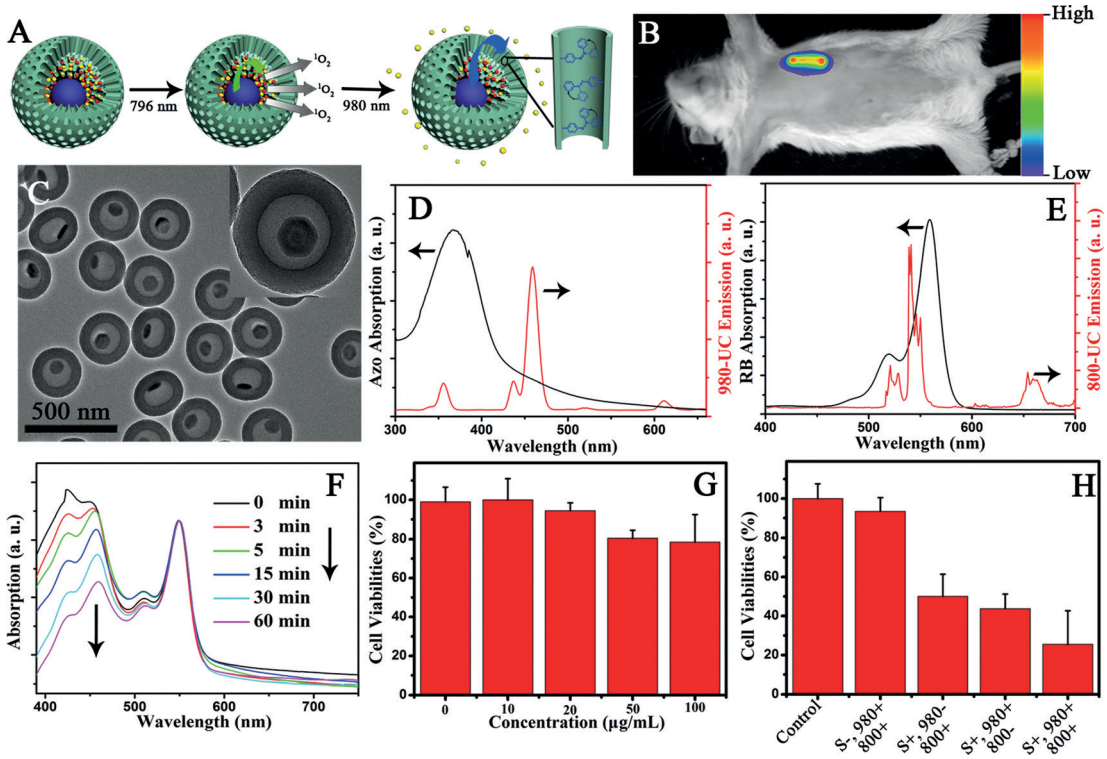

Figure 4. A) Scheme for combined photodynamic therapy and chemotherapy; B) In vivo imaging of a nude mouse with UCNPs@$mSiO_2$ nanocomposites in its stomach under low power density 796 nm excitation; C) TEM image of the UCNPs@$mSiO_2$ nanocomposites; The UV/blue (D) and green (E) UCL of the UCNPs@$mSiO_2$ nanocomposites and the absorption of the UCNPs@$mSiO_2$-Azo (D) and UCNPs@$mSiO_2$-RB (E); F) The time-resolved absorption of DPBF incubated with UCNPs@$mSiO_2$-RB under irradiation of 796 nm; Cell-viability assay of UCNPs@$mSiO_2$ (G) and doxorubicin-loaded UCNPs@$mSiO_2$-RB-Azo (H) under different stimulus (S+: with sample; S−: without sample; 980+, 980− and 800+, 800−: with or without the irradiation of 980 nm or 800 nm light).

(Figure 4E, the absorption matches well with the green emission of the Er^{3+} activator), the released singlet oxygen can be detected by a chemical probe, 1,3-diphenylisobenzofuran (DPBF). The absorption at about 450 nm of DPBF incubated with UCNPs@$mSiO_2$-RB under irradiation of 796 nm gradually decreased with irradiation time (Figure 4F), indicating an increase in the presence of singlet oxygen. The cytotoxicity of this nanocomposite (Figure 4G) shows that the viability of cells is maintained at more than 80% even at a high concentration (ca. 100 $\mu g\,mL^{-1}$), indicating a good biocompatibility of the nanocarrier. In vitro cell cytotoxicity shows that the cancer cells killing efficacy can reach 75% under the irradiation of 980 nm and 796 nm, which is much higher than the single therapeutic model under isolated 980 nm (ca. 55%) or 800 nm (ca. 50%) irradiation.

In summary, filtration shell mediated $NaGdF_4$:Yb,Er@$NaYF_4$:Yb@$NaGdF_4$:Yb,Nd@$NaYF_4$@$NaGdF_4$:Yb,Tm@$NaYF_4$ core-multishell structured UCNPs with power density independent orthogonal excitations-emissions UCL were synthesized for the first time. The optical properties of the UCNPs can be controlled by tuning the thickness of the $NaGdF_4$:Yb,Tm absorption filtration layer. When the thickness of the filtration layer grows up to 15 nm, these core-multishell lanthanide doped nanoparticles can exhibit two independent luminescence events in one nanoparticle: Tm^{3+} UV/blue UCL under 980 nm excitation and Er^{3+} green/red UCL under 796 nm excitation. What is more, the orthogonal excitations-emissions UCL are independent of the power density and ion-doping concentration in each layer. The unique optical properties, allow these core-multishell nanoparticles to be used in multi-dimensional security designs (patterns, emissions, and excitations) and imaging-guided combined therapy. We believe that such a filtration shell mediated strategy for the tuning of the UCL can open the door to extend the optical properties and controllable emissions of core–shell-based lanthanide-doped nanoparticles.

Acknowledgements

The work was supported by China National Key Basic Research Program (973 Project) (No. 2013CB934100 and 2012CB224805), NSFC (grant No. 21322508 and 21210004), Shanghai Shuguang Program, China Postdoctoral Science Foundation (2015M570327).

Keywords: anti-counterfeiting · combined therapy · lanthanides · luminescence · nanoparticles · upconversion

How to cite: *Angew. Chem. Int. Ed.* **2016**, *55*, 2464–2469
Angew. Chem. **2016**, *128*, 2510–2515

[1] a) B. Zhou, B. Shi, D. Jin, X. Liu, *Nat. Nanotechnol.* **2015**, *10*, 924; b) G. Chen, H. Qju, P. N. Prasad, X. Chen, *Chem. Rev.* **2014**, *114*, 5161.

[2] a) X. Chen, D. Peng, Q. Ju, F. Wang, *Chem. Soc. Rev.* **2015**, *44*, 1318; b) Y. Zhong, G. Tian, Z. Gu, Y. Yang, L. Gu, Y. Zhao, Y. Ma, J. Yao, *Adv. Mater.* **2014**, *26*, 2831; c) X. Xie, N. Gao, R. Deng, Q. Sun, Q.-H. Xu, X. Liu, *J. Am. Chem. Soc.* **2013**, *135*, 12608; d) H. Wen, H. Zhu, X. Chen, T. F. Hung, B. Wang, G. Zhu, S. F. Yu, F. Wang, *Angew. Chem. Int. Ed.* **2013**, *52*, 13419; *Angew. Chem.* **2013**, *125*, 13661.

[3] a) N. M. Idris, M. K. G. Jayakumar, A. Bansal, Y. Zhang, *Chem. Soc. Rev.* **2015**, *44*, 1449; b) D. Yang, P. a. Ma, Z. Hou, Z. Cheng, C. Li, J. Lin, *Chem. Soc. Rev.* **2015**, *44*, 1416; c) W. Zheng, P. Huang, D. Tu, E. Ma, H. Zhu, X. Chen, *Chem. Soc. Rev.* **2015**, *44*, 1379.

[4] a) G. Tian, Z. Gu, L. Zhou, W. Yin, X. Liu, L. Yan, S. Jin, W. Ren, G. Xing, S. Li, Y. Zhao, *Adv. Mater.* **2012**, *24*, 1226; b) J. Wang, F. Wang, C. Wang, Z. Liu, X. Liu, *Angew. Chem. Int. Ed.* **2011**, *50*, 10369; *Angew. Chem.* **2011**, *123*, 10553; c) F. Wang, X. Liu, *J. Am. Chem. Soc.* **2008**, *130*, 5642; d) F. Zhang, Q. Shi, Y. Zhang, Y. Shi, K. Ding, D. Zhao, G. D. Stucky, *Adv. Mater.* **2011**, *23*, 3775.

[5] a) J. Lai, Y. Zhang, N. Pasquale, K.-B. Lee, *Angew. Chem. Int. Ed.* **2014**, *53*, 14419; *Angew. Chem.* **2014**, *126*, 14647; b) J.-C. Boyer, C.-J. Carling, B. D. Gates, N. R. Branda, *J. Am. Chem. Soc.* **2010**, *132*, 15766; c) W. Li, Z. Chen, L. Zhou, Z. Li, J. Ren, X. Qu, *J. Am. Chem. Soc.* **2015**, *137*, 8199; d) L. Wang, H. Dong, Y. Li, R. Liu, Y.-F. Wang, H. K. Bisoyi, L.-D. Sun, C.-H. Yan, Q. Li, *Adv. Mater.* **2015**, *27*, 2065.

[6] Q. Dou, N. M. Idris, Y. Zhang, *Biomaterials* **2013**, *34*, 1722.

[7] a) X. Li, D. Shen, J. Yang, C. Yao, R. Che, F. Zhang, D. Zhao, *Chem. Mater.* **2013**, *25*, 106; b) X. Li, R. Wang, F. Zhang, D. Zhao, *Nano Lett.* **2014**, *14*, 3634.

[8] a) J. Zhou, G. Chen, E. Wu, G. Bi, B. Wu, Y. Teng, S. Zhou, J. Qiu, *Nano Lett.* **2013**, *13*, 2241; b) P. Chen, M. Song, E. Wu, B. Wu, J. Zhou, H. Zeng, X. Liu, J. Qiu, *Nanoscale* **2015**, *7*, 6462.

[9] a) J. Lu, E. Choi, F. Tamanoi, J. I. Zink, *Small* **2008**, *4*, 421; b) Y. Zhu, M. Fujiwara, *Angew. Chem. Int. Ed.* **2007**, *46*, 2241; *Angew. Chem.* **2007**, *119*, 2291.

[10] a) J. Liu, W. Bu, L. Pan, J. Shi, *Angew. Chem. Int. Ed.* **2013**, *52*, 4375; *Angew. Chem.* **2013**, *125*, 4471; b) J. Dong, J. I. Zink, *Small* **2015**, *11*, 4165.

[11] G. Chen, T. Y. Ohulchanskyy, S. Liu, W. Law, F. Wu, M. T. Swihart, H. Agren, P. N. Prasad, *ACS Nano* **2012**, *6*, 2969.

Received: November 16, 2015
Published online: January 14, 2016

